View metadata, citation and similar papers at core.ac.uk

brought to you by CORE

provided by Scientific Open-access Literature Archive and Repository

IL NUOVO CIMENTO Vol. 32 C, N. 3-4 Maggio-Agosto 2009
DOI 10.1393/ncc/i2009-10437-1

Colloquia: IFAE 2009

# Search for new physics at BaBar

A. Cervelli on behalf of the BaBar Collaboration

*INFN, Sezione di Pisa - Largo Bruno Pontecorvo 3, I-56127 Pisa, Italy*

(ricevuto il 19 Settembre 2009; pubblicato online il 23 Ottobre 2009)

**Summary.** — We present recent results concerning the searches for light Higgs-like particles in the decay $\Upsilon(3S) \to \gamma A^0$, $A^0 \to \mu^+\mu^-$ and $\Upsilon(3S) \to \gamma A^0$, $A^0 \to$ invisible as well as the latest upper limits measured in the search for lepton flavour violating decays $\tau \to 3\ell$ $(\ell = e, \mu)$ with the BaBar experiment.

PACS `14.60.Fg` – Taus.
PACS `13.35.Dx` – Decays of taus.
PACS `14.80.Ec` – Other neutral Higgs bosons.
PACS `14.80.Va` – Axions and other Nambu-Goldstone bosons (Majorons, familons, etc.).

## 1. – $\Upsilon(3S) \to \gamma A^0$, $A^0 \to \mu^+\mu^-$ and $\Upsilon(3S) \to \gamma A^0$, $A^0 \to$ invisible

The Standard Model of interactions (SM) predicts the existence of a Higgs boson to generate different particle masses. A single SM Higgs boson is expected to be heavy ($m_H > 114.4\,\text{GeV}$) [1], on the other hand, SM suffers from quadratic divergences in the radiative corrections to the Higgs mass parameter. This divergence is fixed through parameter fine tuning in some models, such as the Minimal Supersymmetric Standard Model, but despite solving the divergence problems some issues remain open. A possible solution is to add additional Higgs fields, with one of them expected to be light, as done in the Next-to-Minimal Supersymmetric Standard Model.

Other physical models, motivated by astrophysical observations, predict similar light states. In particular, an axion-like particle $A^0$ decaying predominantly to leptons is predicted by some models [1], with its mass in the range $360\,\text{MeV} \leq m_{A^0} \leq 800\,\text{MeV}$ with a branching ratio (BR) $\Upsilon(3S) \to \gamma A^0$ between $10^{-5}$–$10^{-6}$.

Direct searches constrain $m_{A^0}$ to be below two bottom quark masses, and therefore accessible in $\Upsilon$ decays. A golden channel [1] for this search is $\Upsilon \to \gamma A^0$, with an expected BR as large as $10^{-4}$. CLEO [1] already produced some results with a measured upper limit (UL) for $\Upsilon(1S) \to \gamma A^0(\to \mu^+\mu^-) \approx 4 \times 10^{-6}$ for $m_{A^0} < 2m_\tau$.

Searches for a two-body transition $\Upsilon(3S) \to \gamma A^0$, where $A^0$ is a light scalar particle, with $A^0 \to \mu^+\mu^-$ and $A^0 \to$ invisible have been performed using a data sample of $(121 \pm 1.2) \times 10^6$ $\Upsilon(3S)$ decays recorded by *BaBar* detector. As $\Gamma_{\Upsilon(4S)}/\Gamma_{\Upsilon(3S)} \approx 10^3$,

© Società Italiana di Fisica

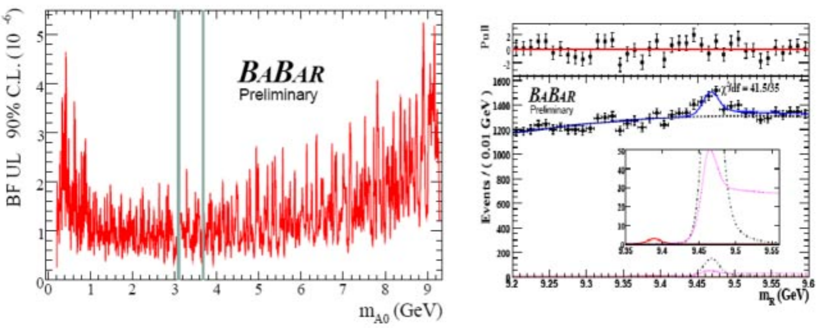

Fig. 1. – (Colour on-line) Left plot: UL for $\mathrm{BR}(\Upsilon(3S) \to \gamma A^0) \times \mathrm{BR}(A^0 \to \mu^+\mu^-)$ as a function of $m_{A^0}$. The shaded areas show the regions around the $J/\psi$ and $\psi(2S)$ resonances excluded from the search. Right plot: the fit for the $\eta_b$ region in $\Upsilon(3S)$ dataset. The bottom graph shows the $m_R$ distribution (solid points), overlaid by the full PDF (solid blue line). The inset shows $e^+e^- \to \gamma_{\mathrm{ISR}}\Upsilon(1S)$ and $\chi_b(2P) \to \gamma\Upsilon(1S)$ in detail. The top plot shows the normalised residuals $p = (data - fit)/\sigma(data)$ with unit error bars.

searches using $\Upsilon(3S)$ data samples achieve better sensitivities than $\Upsilon(4S)$ samples, albeit using only one fifth of the integrated luminosity.

The event selection for $A^0 \to \mu^+\mu^-$ [1] and $A^0 \to$ invisible [2] are described in detail elsewhere. The yield of signal events is extracted as a function of the mass $m_{A^0}$ in the interval $0.212\,\mathrm{GeV} \leq m_{A^0} \leq 9.3\,\mathrm{GeV}$ by performing a series of unbinned extended maximum likelihood fits to the distribution of the "reduced mass"

$$m_R = \sqrt{m_{\mu\mu}^2 - 4m_\mu^2}\,. \qquad (1)$$

The distribution of $m_R$ is such that the main background distribution, represented by $e^+e^- \to \gamma\mu^+\mu^-$ processes produced either from continuum or through ISR-produced $J/\psi$, $\psi(2S)$, $\Upsilon(1S)$ decays, is smooth throughout the entire range of interest. Each fit is performed over a small range of $m_R$ around a particular value of $m_{A^0}$, in total 20 different values of $m_{A^0}$ were tested. The signal PDF is determined with a fit to simulated signal events generated for each different mass point tested. The PDF shape is interpolated between adjacent mass points. Simulation results are calibrated using charmonium backgrounds. The background PDF is determined using $\Upsilon(4S)$ data samples with the same fit procedure performed for the signal.

Almost 2000 $m_R$ points were considered, for each value the significance of any particular peak was determined. The probability to find a $3\sigma$ effect due to statistical fluctuation is of about 80%. The most significant peak is observed at $m_{A^0} = 4.940 \pm 0.003\,\mathrm{GeV}$ ($= 3\sigma$). The second most significant peak is measured at $m_{A^0} = 0.426 \pm 0.001\,\mathrm{GeV}$ ($= 2.9\sigma$). Since no significant excess of events was found above in the range $0.212 < m_{A^0} < 9.3\,\mathrm{GeV}$, it was possible to set ULs on the $\mathrm{BR}(\Upsilon(3S) \to \gamma A^0) \times \mathrm{BR}(A^0 \to \mu^+\mu^-)$ and $\mathrm{BR}(\Upsilon(3S) \to \gamma A^0) \times \mathrm{BR}(A^0 \to \text{invisible})$. The 90% confidence level Bayesian ULs are computed as a function of $m_{A^0}$ assuming a uniform prior and a Gaussian likelihood, results are shown in fig. 1. The limits fluctuate depending on the central value of the signal yield returned by a particular fit, and range between $0.25 \times 10^{-6}$ to $5.2 \times 10^{-6}$ for $A^0 \to \mu^+\mu^-$ and between $0.7 \times 10^{-6}$ to $31 \times 10^{-6}$ for the $A^0 \to$ invisible.

## **2.** – $\tau \to 3\ell$ ($\ell = e, \mu$)

Lepton flavour violation (LFV) involving charged leptons has never been observed, and stringent experimental limits exist from muon BR [3]: $\mathrm{BR}(\mu \to e\gamma) < 1.2 \times 10^{-11}$ and $\mathrm{BR}(\mu \to eee) < 1.0 \times 10^{-12}$ at 90% confidence level (CL). $\tau^- \to \ell^-\ell^+\ell^-$ decays in SM are expected to have BR similar to $\tau \to \mu\gamma$, which are predicted to be $\sim 10^{-54}$ and hence well beyond present (and probably future) experimental sensitivities. Many descriptions of physics beyond the SM, in particular models seeking to describe neutrino mixing, predict enhanced LFV branching fraction in $\tau$ and $\mu$ decays with expected BR for LFV decays ranging from $10^{-10}$ up to the current experimental limits ($10^{-8}$) [3]. An observation of LFV in $\tau$ decays would be a clear signature of new physics, and observing more than one LFV decay mode would shed light on the new physics flavour structure. On the other hand, improved ULs would reduce the parameter space of many theoretical models.

The latest search for the neutrino-less, lepton-flavour violating $\tau$ decay into three charged leptons has been performed using a $470\,\mathrm{fb}^{-1}$ data sample recorded by *BABAR*. All possible lepton combinations consistent with charge conservation are looked for, resulting in a total of six channels under study. This search represents an update of a previous *BABAR* analysis [3], and uses a different selection technique, and improved particle identification algorithms using multivariate analysis tools for electron and muon selection.

In order to reduce background the event is divided into two hemispheres in the $e^+e^-$ centre-of-mass (c.m.) frame using the plane perpendicular to the thrust axis, as calculated from the observed tracks and neutral energy deposits, passing through the interaction region. The signal hemisphere must contain exactly three tracks (each identified as either an electron or muon, with a reconstructed invariant mass and energy compatible with the parent tau lepton), the other (tag) hemisphere must contain exactly one track. All tracks are required to point toward a common region consistent with $\tau^+\tau^-$ production and decay. The three tracks from the signal hemisphere are required to have an invariant mass of less than $3.5\,\mathrm{GeV}/c^2$.

Particle identification (PID) uses new algorithms relative to those used in [4] which improve electron, and in particular muon identification capabilities with respect to the previous analysis. These improvements result in an average efficiency at constant contamination for electrons and muons of 91% and 77%, respectively (older PID had a 65% efficiency for muons). The probability for a pion to be misidentified as an electron in 3-prong tau decays is 2.4%, while the probability to be misidentified as a muon is 2.1%. Older selectors misidentification rates of 2.7% for electrons, and 2.9% for muons.

After PID is applied two variables are defined: $\Delta E \equiv E^\star_{\mathrm{rec}} - E^\star_{\mathrm{beam}}$, where $E^\star_{\mathrm{rec}}$ is the total energy of the tracks observed in the 3-prong hemisphere and $E^\star_{\mathrm{beam}}$ is the beam energy, with both quantities measured in the c.m. frame, and $\Delta M_{ec} \equiv M_{\mathrm{rec}} - m_\tau$ where $M^2_{\mathrm{rec}} \equiv E^{\star\,2}_{\mathrm{beam}}/c^4 - |\vec{p}^{\,\star}_{3l}|^2/c^2$, where $|\vec{p}^{\,\star}_{3l}|^2$ is the squared momentum of the 3-prong tracks in the c.m. and $m_\tau = 1.777\,\mathrm{GeV}/c^2$ is the tau mass. Further background reduction is obtained using topological and kinematic variables (such as the angle between the 3-prong reconstructed momenta and the 1-prong momentum, the missing transverse momentum, and the minimum invariant mass of the two oppositely charged leptons in the 3 prong hemisphere). The selection procedure is blind: for each channel a different rectangular signal box is defined in the $(\Delta E, \Delta M_{ec})$-plane, the dimensions of the signal box are chosen taking into account the smearing caused by experimental resolution and radiative effects. We also define a common large box region, identical for all channels, chosen so that all signal events lie in this region. The expected background events are estimated

TABLE I. – *Signal efficiency, ($N_{\mathrm{bgd}}$), expected branching fraction UL at* 90% *CL ($UL_{90}^{\mathrm{exp}}$), ($N_{\mathrm{obs}}$), measured UL at* 90% *CL ($UL_{90}^{\mathrm{obs}}$) for each decay mode. All upper limits are in units of* $10^{-8}$.

| Mode | Efficiency (%) | $N_{\mathrm{bgd}}$ | $\mathrm{UL}_{90}^{\mathrm{exp}}$ | $N_{\mathrm{obs}}$ | $\mathrm{UL}_{90}^{\mathrm{obs}}$ |
|---|---|---|---|---|---|
| $e^-e^+e^-$ | $8.6 \pm 0.2$ | $0.12 \pm 0.02$ | 3.4 | 0 | 2.9 |
| $\mu^-e^+e^-$ | $8.8 \pm 0.5$ | $0.64 \pm 0.19$ | 3.7 | 0 | 2.2 |
| $\mu^+e^-e^-$ | $12.7 \pm 0.7$ | $0.34 \pm 0.12$ | 2.2 | 0 | 1.8 |
| $e^+\mu^-\mu^-$ | $10.2 \pm 0.6$ | $0.03 \pm 0.02$ | 2.8 | 0 | 2.6 |
| $e^-\mu^+\mu^-$ | $6.4 \pm 0.4$ | $0.54 \pm 0.14$ | 4.6 | 0 | 3.2 |
| $\mu^-\mu^+\mu^-$ | $6.6 \pm 0.6$ | $0.44 \pm 0.17$ | 4.0 | 0 | 3.3 |

fitting the MC and data in the sideband region (defined as the region of the large box not including the signal box). Cross checks have been performed to validate the fit, by looking at expected and observed background events in the sideband regions adjacent to the signal box.

The numbers of events observed ($N_{\mathrm{obs}}$) and the background expectations ($N_{\mathrm{bgd}}$) in the signal box are shown in table I: no events were found in the signal box for all channels. ULs on the branching fractions are calculated using Cousin and Highland method [5] with Barlow implementation. The main sources of systematic uncertainties are represented by the uncertainty on the number of $\tau$-pairs produced, which is estimated to be 0.9%, uncertainties on the selection efficiency, dominated by the PID efficiency error in the 3-prong hemisphere, and uncertainties on the number of expected background events, which are dominated by the choice of the shapes used to model the MC distributions in the $(\Delta M_{ec}, \Delta E)$-plane. The sensitivity or expected upper limit $\mathrm{UL}_{90}^{\mathrm{exp}}$, defined as the mean upper limit expected in the background-only hypothesis, is included in table I. The 90% CL ULs for $\tau^- \to \ell^-\ell^+\ell^-$ BR are measured to be in the range $(1.8–3.3) \times 10^{-8}$. This analysis supersedes the previous *BABAR* analysis [3], and also represents also an improvement with respect to the previous experimental bounds [6], obtaining smaller UL for $e^-e^+e^-$, $\mu^-e^+e^-$, $\mu^+e^-e^-$, and $e^-\mu^+\mu^-$ channels. This analysis has improved the UL by a factor $\approx$ 5–8 with only a small increase in luminosity thanks to the use of new tools and new event selections.

## 3. – Conclusion

The high luminosity delivered by PeP-II and the excellent efficiency of *BABAR* detector made it possible to make searches for new particles and rare processes with unprecedented sensitivities. The results on $A^0$ Higgs-like or axion-like particles searches reached better sensitivities with respect to the previous CLEO searches, over an even wider range of masses, in the searches for LFV $\tau$ best present UL were set for four of the six channels under study, despite the smaller integrated luminosity with respect to Belle.

REFERENCES

[1] AUBERT B. *et al.* (BABAR COLLABORATION), arXiv:hep-ex/0812.1021v2.
[2] AUBERT B. *et al.* (BABAR COLLABORATION), arXiv:hep-ex/0808.0017v1.
[3] AUBERT B. *et al.* (BABAR COLLABORATION), *Phys. Rev. Lett.*, **99** (2007) 251803.
[4] AUBERT B. *et al.* (BABAR COLLABORATION), to be published soon.
[5] FELDMAN G. J. and COUSINS R. D., *Phys. Rev. D*, **57** (1998) 3873.
[6] MIYAZAKI Y. *et al.* (BELLE COLLABORATION), *Phys. Lett. B*, **660** (2008) 154.